B17

Damage assessment of urban areas due to the 2015 Nepal earthquake using TerraSAR-X imagery

○Rendy Bahri[1], Wen Liu[2], Fumio Yamazaki[2]

Abstract: The 2015 Gorkha, Nepal, earthquake with Mw 7.8 occurred on April 25, 2015. Many buildings including the world heritages in three Durbar Squares collapsed by this event. Satellite remote sensing is recognized as an effective tool for detecting and monitoring affected areas due to natural disasters. In this study, we used two-temporal high-resolution TerraSAR-X images to detect the changes of urban areas in Kathmandu, the capital city of Nepal. TerraSAR-X images obtained before and after the earthquake were utilized for calculating the difference and correlation coefficient of the SAR backscatter. The mean texture of the Gray-Level Co-occurrence Matrix (GLCM) was also introduced in order to improve the accuracy of extracting damaged buildings in the central Kathmandu.

Keywords: The 2015 Nepal Earthquake, TerraSAR-X, damage assessment, Texture, GLCM

1. Introduction

The 2015 Gorkha earthquake with Mw 7.8 occurred at 11:56 NST on 25 April in the central part of Nepal. A major aftershock with Mw 6.7 followed on 26 April 2015 in the same region at 12:55 NST. Due to the earthquake, centuries-old buildings were destroyed at UNESCO World Heritage sites in the Kathmandu Valley, including some at the Kathmandu Durbar Square. In order to grasp damage situation quickly after a natural disaster strikes, remote sensing is recognized as an effective tool. Especially, Synthetic Aperture Radar (SAR) sensors can observe objects on the earth surface without depending on the sunlight condition and under cloud-cover. Recently, the texture analysis of remotely sensed imagery becomes popular especially in land-cover classification.

In this study, TerraSAR-X images obtained before and after the Nepal earthquake are used for detecting damaged buildings in Kathmandu. In order to get a better result, texture features of the SAR images are tested.

2. The study area and imagery data used

Kathmandu, the capital and largest municipality of Nepal, was selected as the study area of this paper as shown in **Fig. 1**. Especially we focused on the central Kathmandu including the Durbar Square, one of the World heritage sites in Nepal.

In this study we used the images obtained by TerraSAR-X that was launched on 2007 by the German Aerospace Center (DLR). A pre-event SAR image was acquired on October 13, 2013 and a post-event image was acquired on April 27, 2015 (2 days after the earthquake). The acquisition mode of the images was Spotlight with VV polarization and an incidences angle of 39.5 degrees. **Fig. 2** shows a color composite of the pre- and post-event images, in which several changed areas could be confirmed by red (increased backscatter) and cyan (decreased backscatter) colors. The blue square shows the study area. Radiometric calibration for each intensity image was carried out to get the backscattering coefficient (sigma naught, σ^0). After this conversion, two pre-processing steps were applied. First, an adaptive filter[1)] was applied to the original SAR images to reduce the speckle noise in order to get the differences and

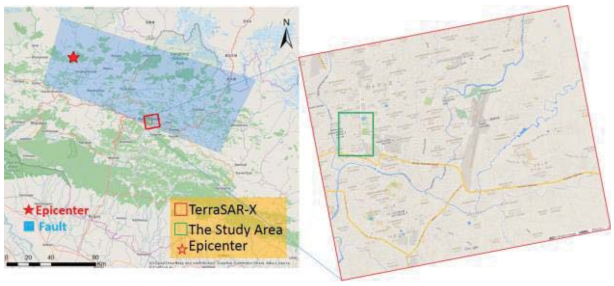

Fig. 1 The Study area of the 2015 Nepal earthquake

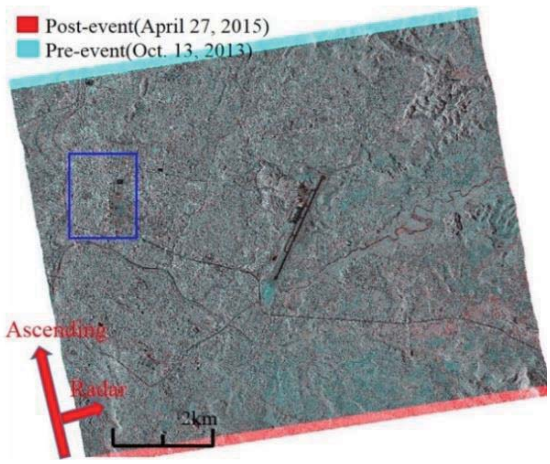

Fig. 2 Color composite of TerraSAR-X images in Kathmandu and the target area (blue square)

[1]Graduate Student, Department of urban Environment Systems, Chiba University
1-33 Yayoi-cho, Inage-ku, Chiba 263-8522, Japan. E-mail: rendy.bahri@gmail.com
[2] Member, Department of urban Environment Systems, Chiba University

correlation coefficient. Second, according to visual comparison, the texture feature (GLCM Mean)[2] in Eq. (1) was applied to in order to get a better result.

$$AVER = \sum_{k=0}^{2G-2} iPx + y(i) \qquad (1)$$

where G (=32) is the number or grey levels used. Angle 0° and radius 1pixel were chosen and a window size of 11 X 11 was used in calculating the texture. The same windows size was also used in obtaining the difference and correlation coefficient.

Two optical satellite images were also introduced as validation data: a pre-event WorldView-3 image on October 14, 2014 and a post-event GeoEye-1 image on May 15,2015, as shown in **Fig. 3**(d)-(f).

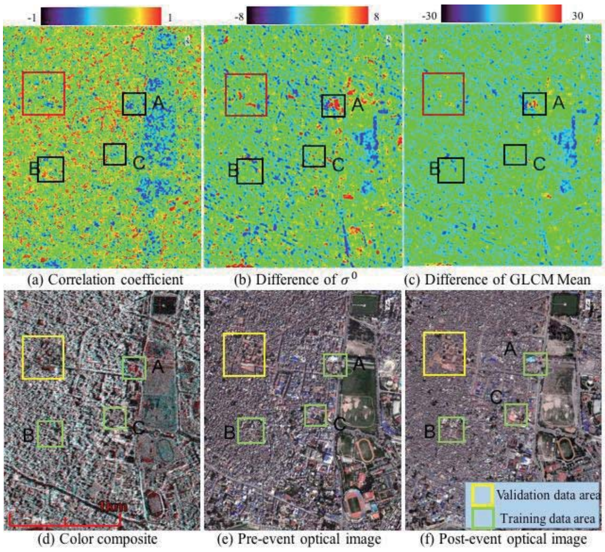

Fig. 3 Close-up of the central Kathmandu: (a) Correlation coefficient; (b) Difference; (c) Z-Factor; (d) Color composite of the TSX images with the post-event (red) and pre-event (blue + green: cyan) ones; (e) the pre-event WV-3 image on October 14, 2014; (f) the post-event GE-1 image on May 15, 2015.

3. Method of damage detection

The change detection from two-temporal SAR intensity images can be evaluated quantitatively by the correlation coefficient *(r)* and their backscattering difference value (*d*), calculated from Eqs. (2) and (3). An 11×11 pixels' window was adopted to obtain *d* and *r* in this study.

The results of the correlation coefficient and difference without texture and the difference of the GLCM mean textures are shown in **Fig. 3**(a)-(c). In the figure, the green color squares show the training data areas that will be discussed later while the yellow square is the validation data area (Durbar square), shown in **Fig. 4**. In this figure, the red lines show collapsed buildings and yellow lines show severely damage buildings. Note that break lines indicate the footprint of a building and solid lines the layover area of a building due to the oblique incidence of radar. The length of layover was calculated by Eq. 4, in which H is the estimation height of a building and θ is the SAR incidence angle. These validation data area were made by observing optical images, field survey photos, the truth map, a drone aerial video[3], as shown in **Fig. 5**. This validation area will be used to choose the threshold for possibly damaged areas.

$$r = \frac{N\sum_{i=1}^{N} Ia_i Ib_i - \sum_{i=1}^{N} Ia_i \sum_{i=1}^{N} Ib_i}{\sqrt{\left(N\sum_{i=1}^{N} Ia_i^2 - \left(\sum_{i=1}^{N} Ia_i\right)^2\right)\cdot\left(N\sum_{i=1}^{N} Ib_i^2 - \left(\sum_{i=1}^{N} Ib_i\right)^2\right)}} \qquad (2)$$

$$d = \bar{I}a_i - \bar{I}b_i \qquad (3)$$

$$L = \frac{H}{\tan\theta} \qquad (4)$$

Fig. 4 Verification data in the Durbar Square

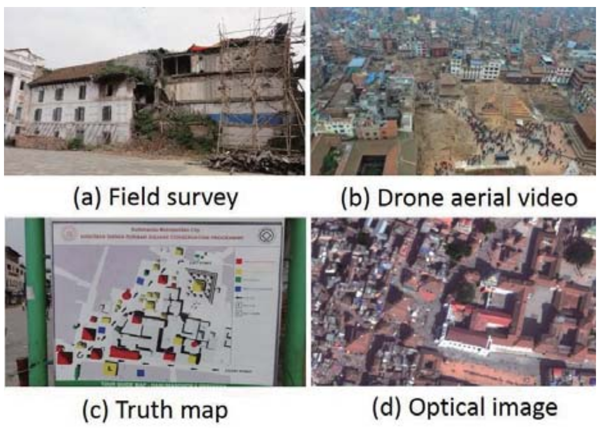

Fig. 5 Reference data used for verification: (a) a field survey photo, (b) a snapshot of the drone aerial video, (c) the truth map made by the Government, (d) a WorldView-3 image.

In this study, we used a trial-anderrors method to choose the threshold for extracting damaged areas due to the earthquake. First we tried to change the correlation coefficient from 0.16, the result of our previous study[4], and next 0.0 to -0.4 with 0.05 interval. Secondly, the best combination between the correct detection and missed detection was selected in the validation area. Finally, the the best threshold of the correlation coefficient was determined as less than -0.20, as shown in **Fig. 6.** The same method was used to decide the difference without texture and when applying the texture difference. The threshold of the difference without texture was smaller than -5.5 dB and bigger than 5.5 dB (|d|≧5.5 dB), as shown in **Fig. 7(a)**. The threshold when applying the texture difference was set as smaller than -20 dB and bigger than 20 dB (|d`|≧20 dB), as shown in **Fig. 7(b)**.

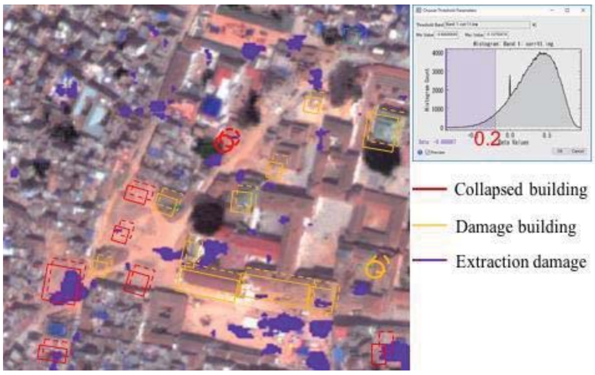

Fig. 6 Trial-and-error to find the threshold (r<-0.2)

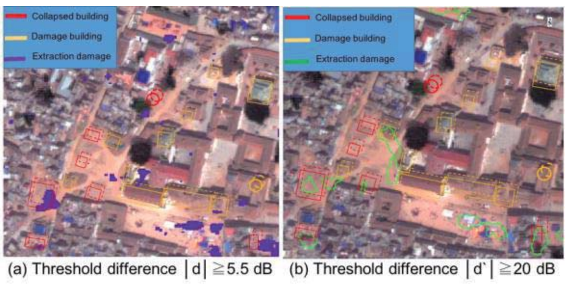

Fig. 7 Extracted areas from different threshold values

4. Detection Result

In this study, we would like to compare the results among the use of the correlation coefficient or the difference without texture, and that when applying the texture difference. As shown in **Fig. 3**, we chose three areas that were possibly changed after the earthquake, such as the area A shown in **Fig. 8**. Changed buildings shown by red color were extracted visually from the pre- and post-event optical images. This building was not destroyed due to the earthquake but some new buildings were under construction in the area. From **Fig. 8**, we can observe that the extraction result by the correlation coefficient is quite good, with very small miss extraction.

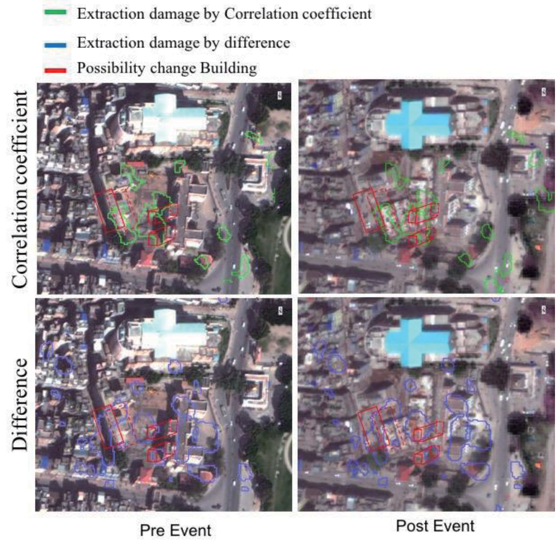

Fig. 8 Extraction result from the correlation coefficient and difference of σ^0 values for the area A

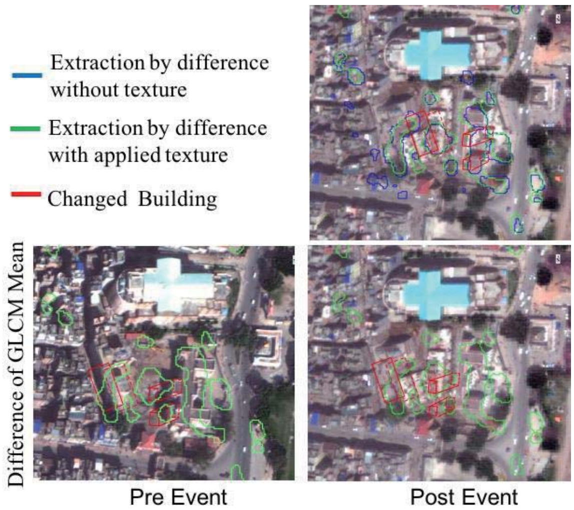

Fig. 9 Extraction results for the difference with and without texture for the area A

The miss extraction was almost in vegetation or on roads, affected by the movement of cars. On the contrary, the extraction result by the difference was not as good as that by the correlation coefficient; miss-extraction was seen in some buildings. But a part of changed areas was extracted well. The result by applying texture difference is better, compared with the other cases as shown in **Fig. 9**. Some noises and miss extraction are still seen, but they look less than the case from the difference without texture. But in some parts, missed extraction is still many seen.

For the area C, shown in **Fig. 10**, the extraction result of difference without texture was located only close to the tower, but the rubble of the destroyed tower fell down to the south of the tower, as seen in the bottom figure. On the other hand, the result from the difference with texture (GLCM Mean) could capture the rubble location.

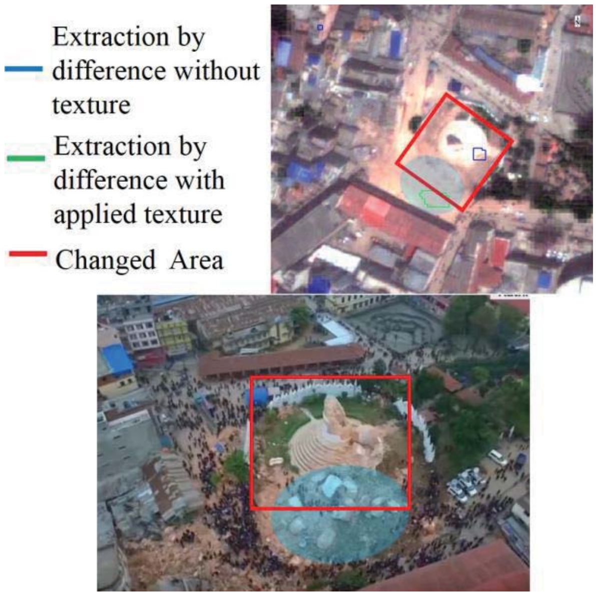

Fig. 10 Extraction result for difference with and without texture for the area B

Lastly the extraction of possible changed/damaged buildings due to the earthquake was carried out for the whole study area, as shown in **Fig. 11**. The extraction result of changed areas by the correlation coefficient for the entire area looks good, but many missed detections exist. On the other hand, the extraction result by the difference is less, compared with that from the correlation coefficient. There are many extractions from the correlation coefficient while only few from the difference in the right side of the area A. This may be caused by the change of vegetation, which affects the SAR backscatter and makes the correlation coefficient lower while the change is quite small and thus not detected by the difference.

Finally, the results with and without texture were compared in **Fig. 11**, where the number of extracted pixels is less using texture (GLCM Mean) and missed extraction also decreased for the truth result. Although the accuracy of these three cases was not evaluated quantitatively, the use of texture measures has possibility to improve the damage extraction accuracy in urban areas.

5. Conclusion

The pre- and post-event high-resolution TerraSAR-X images were used to assess the damages in the urban areas due to the 2015 Nepal earthquake. The affected areas were estimated according to a multi-temporal color composite, and the difference and correlation coefficient of the sigma naught value. Texture measures were also introduced to improve the accuracy of damage extraction.

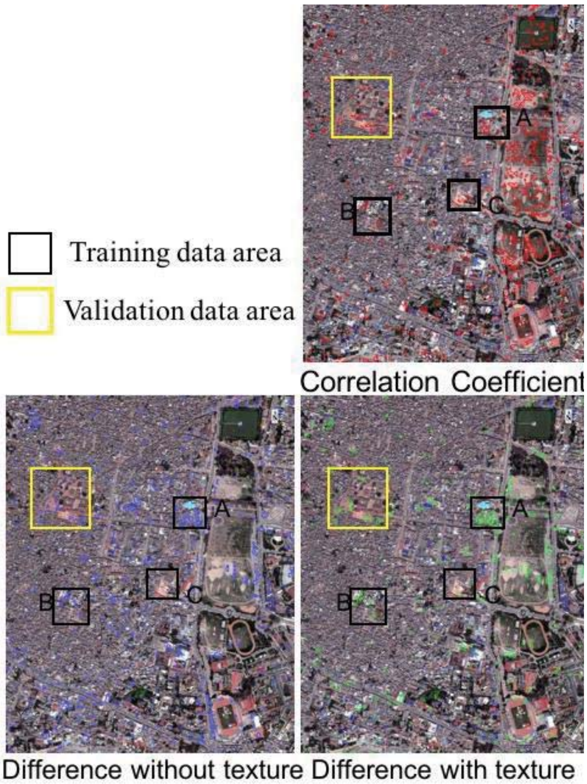

Fig. 11 Extraction result for the whole study area

The results from these methods were compared with high-resolution optical images. The results showed that by introducing a texture measure (GLCM Mean), the accuracy of damaged areas look to be improved. Although it was still difficult to estimate the damage level of individual buildings, but the high-resolution SAR images illustrated their capability in emergency response.

Acknowledgement: The TerraSAR-X data are the property of the German Aerospace Center (DLR) and Infoterra GmbH and were made available by the PASCO Corporation, Tokyo, Japan.

References

1) Lee, J.S., Digital image enhancement and noise filtering by use of local statistics, IEEE Transaction on Pattern Analysis and Machine Intelligence, 2(2), 165-168, 1980.

2) Haralick, R.M., Shanmugam, K., Dinstein, I., Textural Features for Images Classification, IEEE Transactions On Systems, Man and Cybernetics, Vol.SMC-3, No.6, pp.610-621,1973.

3) YouTube: Drone footage captures aftermath of Nepal Earthquake. https://www.youtube.com/watch?v=N52LX1GZYWs

4) Bahri, R., Liu, W., Yamazaki, F., and Sasagawa, T., Damage assessment of buildings in Kathmandu due to the 2015 Nepal earthquake using TerraSAR-X imagery, 60th RSSJ, 15-18, 2016. (In Japanese)